

MULTIPACTING SIMULATIONS OF TTF-III POWER COUPLER COMPONENTS**

L. Ge¹, C. Adolphsen, L. K. Ko, Lee, Z. Li, C. Ng, G. Schussman, F. Wang, SLAC, Menlo Park, CA 94025;
B. Rusnak, LLNL, Livermore, CA 94550

Abstract

The TTF-III power coupler adopted for the ILC baseline cavity design has shown a tendency to have long initial high power processing time. A possible cause for the long processing time is believed to be multipacting in various regions of the coupler. To understand performance limitations during high power processing, SLAC has built a flexible high-power coupler test stand. The plan is to test individual sections of the coupler, which includes the cold and warm coaxes, the cold and warm bellows, and the cold window, using the test stand to identify problematic regions. To provide insights for the high power test, detailed numerical simulations of multipacting for these sections will be performed using the 3D multipacting code Track3P.

INTRODUCTION

The power coupler designs for the ILC main linac cavities are complex devices due to the required cleanliness, temperature gradient, vacuum isolation and tunability requirements. During high power tests, the ILC baseline TTF-III coupler experienced long processing time [1]. To better understand the rf processing limitations of the coupler, SLAC, in collaboration with LLNL, has built a flexible high-power test stand [2]. Various coupler sections will be tested to assess the impact of coatings, bellows, and windows on the rf processing time [3].

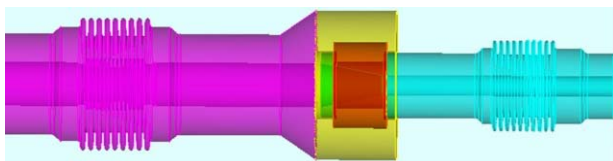


Figure 1: Model of the TTF-III power coupler. The ceramic window near the center separates the cold and warm regions with coaxes and bellows.

A possible cause for the long processing time is believed to be multipacting in various parts of the coupler. The coupler comprises of different components including the cold/warm coaxes, the cold/warm bellows and the ceramic window separating the cold and warm sides. A model of the TTF-III coupler is shown in Fig. 1. These components will be inserted in the test stand separately for high power processing. Because of the differences in

coax dimensions of the coupler components, the test stand included two taper adaptors to match to the components of different dimensions. To corroborate with experimental measurements, numerical simulations of multipacting for individual components will be carried out, so possible problematic regions may be identified. The possibility of multipacting activities in the matching taper will be analyzed through simulations, which will help identify if the test component contributes to the observed multipacting signals during high power processing.

MULTIPACTING ANALYSIS

Simulations of multipacting for the coupler components have been carried out using Track3P. Track3P is a 3D particle tracking code in electromagnetic fields using the finite-element method. The finite element grid with curved elements fitted to the curvature of the boundary allows high-fidelity modeling of the geometry and, in the case of particle tracking, correct emission angles for particles with respect to the surface curvature. Several emission models for thermal, field and secondary emissions have been implemented in Track3P. It can trace particle trajectories in structures excited by resonant modes, steady state or transient fields, which are taken as input obtained by a field solver. Track3P has been extensively benchmarked against measurements for dark current and multipacting [4, 5]. Recently, it has been used to predict correctly the multipacting barriers in the ILC ICHIRO cavity [6].

In a typical multipacting simulation, electrons are launched from specific surfaces at different phases over a full rf period. The initial launched electrons follow the electromagnetic fields in the structure and eventually hit the boundary, where secondary electrons are emitted based on the secondary emission yield (SEY) of the surface material. The tracing of electrons will continue for a specified number of rf cycles, after which resonant trajectories are identified. Not all of these resonant trajectories contribute to multipacting. Only those with successive impact energies within the right range for secondary emission yield bigger than unity will be treated as multipacting events. We have written a postprocessing tool in Track3P for the effective extraction of these events. The tool also enables to determine the multipacting order and type, which are

*Work supported by the U.S. DOE ASCR, BES, and HEP Divisions under contract No. DE-AC02-76SF00515. The work used the resources of NCCS at ORNL which is supported by the Office of Science of the U.S. DOE under Contract No. DE-AC05-00OR22725, and the resources of NERSC at LBNL which is supported by the Office of Science of the U.S. DOE under Contract No. DE-AC03-76SF00098.

#This work was performed under the auspices of the U. S. Department of Energy by the University of California, Lawrence Livermore National Laboratory under Contract No. W-7405-Eng-48.

¹lge@slac.stanford.edu

defined as the number of cycles per impact and the number of impacts per multipacting cycle, respectively.

To identify possible multipacting barriers during processing for the TTF-III coupler, we scan the input power up to 1 MW with a 50 kW interval. In the following, we will present simulation results for the cold coax, cold bellows, ceramic window and the taper.

SIMULATION OF COAX

The first component of the TTF-III power coupler tested for high power processing is the cold coax. Fig. 2 shows a model of the coax in the experimental setup. In addition to monitoring vacuum pressure during processing, an electron pickup is placed on the outside wall of the coax to measure electron signals. Note that matching tapers are connected at each end of the coax. In this section, we focus on the multipacting analysis in the coax, and defer that in the taper region to a later section.

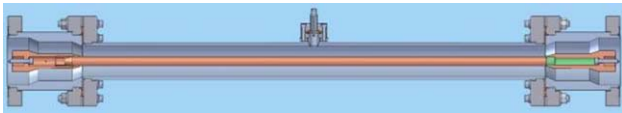


Figure 2: Model of the coax in the test stand.

There exists theoretical analysis of multipacting in coaxial lines. In Ref. [7], scaling laws relating the power level for the occurrence of multipacting to the coax geometry and rf frequency were derived for 1-point and 2-point multipacting. Multipacting also occurs as different bands depending on the multipacting order. In a given geometry driven at a certain frequency, the multipacting events at lower power levels are more likely of higher orders. We have used Track3P to determine the multipacting bands of the coupler coax for both cases of traveling wave and standing wave, and obtained excellent agreement with the scaling laws with respect to both the multipacting power level and the multipacting order.

The calculated multipacting bands and the measured electron pickup and vacuum signals after initial processing for the cold coax component exhibit good agreement as shown in Fig. 3. Table 1 lists the power levels for the occurrences of different multipacting bands. The klystron and coupler powers monitored during experiments are different because of attenuation in the setup.

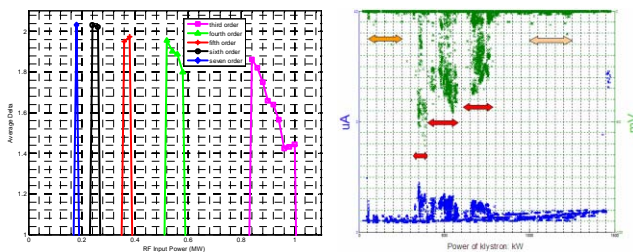


Figure 3: (Left) Simulated and (Right) measured multipacting bands in the cold coax.

Table 1: Power levels (in kW) for the occurrences of multipacting in the cold coax.

| Simulation | 170-190 | 230-270 | 350-390 | 510-590 | 830-1000 |
|------------|---------|---------|---------|---------|-----------|
| Coupler | 43-170 | 280-340 | 340-490 | 530-660 | 850-1020 |
| Klystron | 50-200 | 330-400 | 400-580 | 620-780 | 1000-1200 |

During the transient of cavity filling, the input power is partially reflected which forms a partial standing wave in the coupler. The transient reflection ranges from 1 to 0 in the matched case. Thus it is instructive to investigate how the multipacting behaviors in the coupler change with finite reflections. Fig. 4 shows the multipacting maps for the cold coax indicating the dependence of multipacting order on the power level for the cases with reflection coefficient 0 and 0.5, respectively. In general, the multipacting order decreases at higher power levels. When a partial standing wave exists in the coax, multipacting is shifted towards lower orders and lower power levels. Fig. 5 shows a multipacting trajectory for the reflection of 0.5. It is a 5th order multipacting event at the power level of 160 kW, and has an impact energy of 543 eV which falls in the enhancement portion of the SEY curve for niobium.

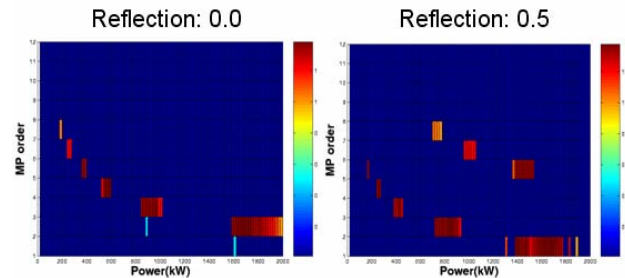


Figure 4: Multipacting maps of the coax for reflection coefficients of 0 and 0.5.

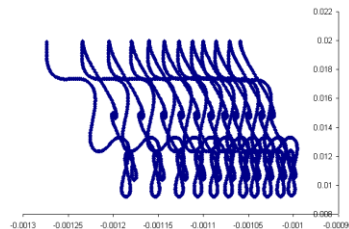


Figure 5: Multipacting trajectory in the coax, with the horizontal and vertical axes being the z and r coordinates.

SIMULATION OF BELLOWS

The simulation of the cold bellows region includes the cold bellows and the coax at both ends because the coax is required for the propagation of a traveling wave. There were no multipacting activities observed in the bellows region up to 1 MW of input power. Fig. 6 shows electron distributions at the 2nd and the 100th rf period. No electrons “survived” longer than 100 rf periods in the bellows region, but multipacting activities remain in the upstream and downstream coax regions as has been discussed in details in the last section.

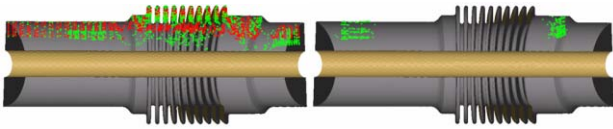


Figure 6: Electron distribution in the bellows at (Left) 1st rf period and at (Right) 100th rf period with initially launched and secondary electrons in red and green, respectively.

SIMULATION OF CERAMIC WINDOW

Because of the lack of measured data on secondary emission yield of ceramic surface, we cannot use the SEY enhancement factor to quantify multipacting events. Instead we use the impact energy to indicate multipacting activities when resonant trajectories are detected [8]. Fig. 7 shows the electric field pattern in the region near the ceramic window. A 2-point multipacting event is shown between the ceramic window and the inner conductor on the cold side. Fig. 8 shows the multipacting map for the possible occurrences of multipacting bands as a function of power level.

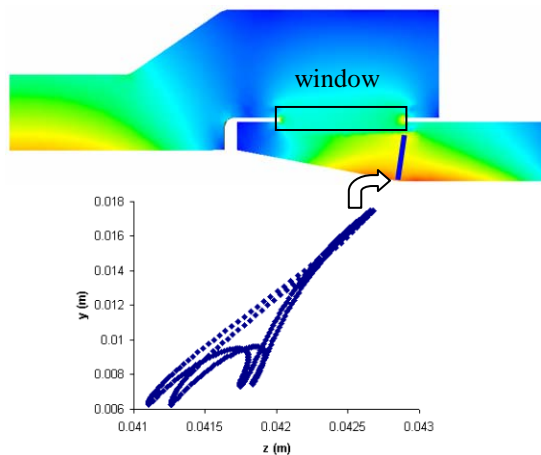


Figure 7: A two-point multipacting trajectory between the ceramic window and the inner conductor of the coax.

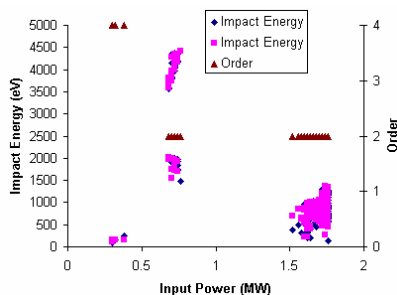


Figure 8: Impact energy and multipacting order as a function of power level for the ceramic window.

SIMULATION OF TAPER

In order to obtain a correct and definite account of the pickup signal when processing a test component, the multipacting behaviors of the taper region need to be elucidated. Fig. 9 shows the multipacting map in the taper region. It is interesting to notice that no multipacting

activities occur in the tapering steps, and multipacting bands exist in the coax sections as expected. It is desirable to suppress multipacting activities in the taper region so any such activities observed during processing can solely be attributed to the test component. It was found from simulations that the suppressing of multipacting in the taper region can be achieved by applying an axial magnetic field above 360 Gauss.

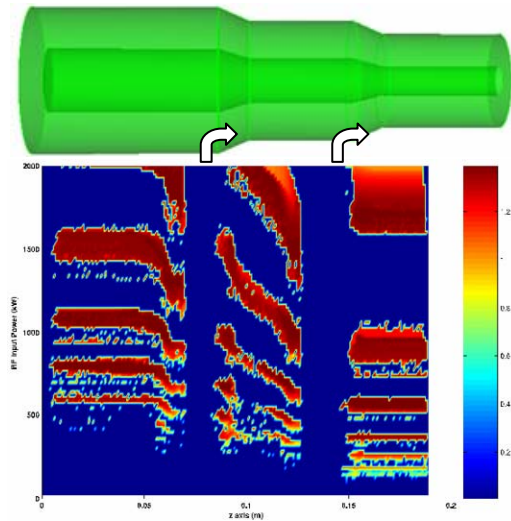


Figure 9: Multipacting activities in the taper region. The bottom picture shows the multipacting map as a function of the longitudinal position along the taper region.

SUMMARY

We have simulated multipacting for various components of the TTF power coupler. The simulated multipacting bands agree well with theoretical calculations and experimental measurements for the cold coax. Simulations results will be used to corroborate with high power test studies for other coupler components and for possible modifications to reduce the processing time.

REFERENCES

- [1] H. Jenhani et al., "Developments in Conditioning Procedure for the TTF-III Power Couplers", Proc. EPAC 2006, Edinburgh, Scotland.
- [2] Brian Rusnak, et al., "High-Power Coupler Component Test Stand Status and Results", these proceedings.
- [3] C. Adolphsen, "ILC Linac R&D at SLAC", Proc. EPAC 2006, Edinburgh, Scotland.
- [4] C.-K. Ng et al., "Simulating Dark Current in NLC Structures", Nucl. Instru. Meth. A558, 192 (2006).
- [5] Z. Li et al., "Towards Simulation of Electromagnetics and Beam Physics at the Petascale", these proceedings.
- [6] C.-K. Ng et al., "State of the Art in EM Field Computation", Proc. EPAC 2006, Edinburgh, Scotland.
- [7] E. Somersalo and P. Yla-Oijala, "Analysis of Multipacting in Coaxial Lines", Proc. PAC 1995, Dallas, Texas.
- [8] T. Abe et al., "Multipactoring Zone Map of an RF Coupler and its Application to High Beam Current Storage Rings", Phys. Rev. STAB, 9, 062002 (2006).